

## Nonequilibrium System as a Demon

Rafael Sánchez<sup>1</sup>, Janine Splettstoesser<sup>2,\*</sup> and Robert S. Whitney<sup>3</sup><sup>1</sup>Departamento de Física Teórica de la Materia Condensada, Condensed Matter Physics Center (IFIMAC), and Instituto Nicolás Cabrera, Universidad Autónoma de Madrid, 28049 Madrid, Spain<sup>2</sup>Department of Microtechnology and Nanoscience (MC2), Chalmers University of Technology, S-412 96 Göteborg, Sweden<sup>3</sup>Laboratoire de Physique et Modélisation des Milieux Condensés, Université Grenoble Alpes and CNRS, BP 166, 38042 Grenoble, France (Received 13 November 2018; published 19 November 2019)

Maxwell demons are creatures that are imagined to be able to reduce the entropy of a system without performing any work on it. Conventionally, such a Maxwell demon's intricate action consists of measuring individual particles and subsequently performing feedback. We show that much simpler setups can still act as demons: we demonstrate that it is sufficient to exploit a nonequilibrium distribution to *seemingly* break the second law of thermodynamics. We propose both an electronic and an optical implementation of this phenomenon, realizable with current technology.

DOI: 10.1103/PhysRevLett.123.216801

**Introduction.**—The second law of thermodynamics requires entropy to increase on long timescales. Maxwell demons apparently break this law by decreasing the entropy in a system without transferring any energy to it [1]. They do this by measuring individual particles and performing feedback based on the information acquired. The second law is restored [2] by the Maxwell demon generating entropy when erasing the information it has acquired about the system [3]. Even though highly intricate, such Maxwell demons have been built in electronic [4–7], superconducting [8,9], and optical [10] systems, using NMR [11], and optically or electrically controlled molecules [12] or microscopic objects [13–15].

This Letter shows that a much simpler class of setups has an analogous effect *without* involving any measurement of individual particles (namely, avoiding any acquisition of information), or any feedback, but instead exploiting a nonequilibrium ( $N$ ) distribution. In this sense such a setup is different from a typical Maxwell demon, and we call it an  $N$ -demon. This  $N$ -demon induces a *steady-state* reduction of the expectation value of the entropy of a pair of reservoirs,  $\dot{S}_1 + \dot{S}_2 < 0$ , without any steady-state supply of heat, work, or other energy. We consider two examples of this entropy reduction: (i) heat in reservoirs 1 and 2 is turned into work when the two reservoirs are at the same temperature, generating electrical (or electrochemical) power while cooling these reservoirs, and (ii) heat is moved from reservoir 1 to 2, where reservoir 1 is colder. These are, respectively, apparent violations of the Kelvin and Clausius versions of the second law. An example of such a  $N$ -demon is shown in Fig. 1(a). This demon injects a nonequilibrium distribution of particles symbolized by a pair of faucets inserting particles from cold (blue) and hot (red) distributions, at rates chosen so that they carry the same average

energy as the backflow of particles (magenta). This way, there is no steady-state particle or energy flow between the  $N$ -demon and the working substance. In other words, there is no flow of heat or work. We propose straightforward implementations of such  $N$ -demons in both electronic and

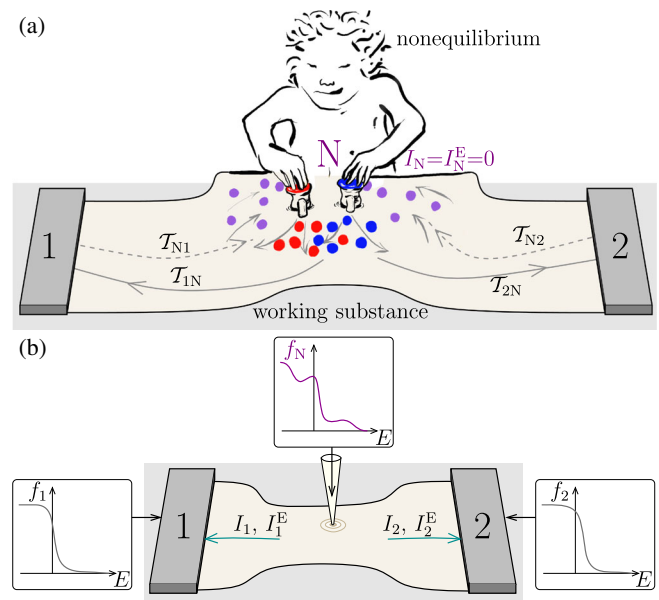


FIG. 1. (a) The  $N$ -demon supplies no heat or work, but it supplies a nonequilibrium distribution to the working substance containing equilibrium reservoirs 1 and 2. The nonequilibrium distribution could be a nonthermalized mixture of different equilibrium distributions. Transmission probabilities,  $\mathcal{T}_{ij}$ , of the scattering region (beige) involving terminal  $N$  are indicated and accompanied by gray arrows. (b) A physical implementation in which the nonequilibrium distribution  $f_N$  is injected locally into the working substance.

optical systems, and we show that they do not violate the second law.

*General entropic analysis.*—Consider the three-terminal setup in Fig. 1, where our aim is that terminal  $N$  [16] (the  $N$ -demon) reduces the entropy of the working substance (always indicated with a gray background) containing reservoirs 1 and 2. We are interested in exploiting terminal  $N$ 's nonequilibrium distribution as the resource, unlike traditional thermodynamics which exploit heat as the resource. To clarify the effect of the nonequilibrium distribution alone, we will concentrate on cases where terminal  $N$  supplies no heat or work to reservoirs 1 and 2; we will call this the “demon conditions” below.

We assume reservoirs 1 and 2 are each in internal equilibrium, so the rate of entropy change in each is given by a Clausius relation  $\dot{S}_i = J_i/T_i$ , where  $J_i$  is the heat current into reservoir  $i = 1, 2$ , which has temperature  $T_i$ . For particles in the presence of an electrochemical potential  $\mu_i$ , the heat current is  $J_i = I_i^E - \mu_i I_i$ , with the particle current  $I_i$  and the energy current  $I_i^E$  [17,18]. However, as  $N$  is out of equilibrium, there is no such relationship for  $\dot{S}_N$ . The second law of thermodynamics is

$$0 \leq \dot{S}_N + J_1/T_1 + J_2/T_2. \quad (1)$$

The demon conditions in which the  $N$ -demon neither injects nor extracts heat or work are  $I_N^E = I_N = 0$ . If the  $N$ -demon were in internal equilibrium, it too would obey a Clausius relation, so these conditions would fix  $\dot{S}_N = 0$ . Then Eq. (1) would become the usual second law for two reservoirs, forbidding the reduction of the sum of their entropies. However, one can have  $\dot{S}_N \neq 0$  under demon conditions if terminal  $N$  is out of equilibrium.

Take example (i) above, with reservoirs 1 and 2 at the same temperature  $T$ , but with  $\mu_1 \neq \mu_2$ . The second law in Eq. (1) becomes  $P = (\mu_1 - \mu_2)I_1 \leq T\dot{S}_N$ , where  $P$  is the electrical power output. Thus if  $\dot{S}_N$  is positive, the working substance is allowed to do work (positive  $P$ ) even when the  $N$ -demon supplies no work or heat,  $I_N^E = I_N = 0$ . This means the work output comes from a reduction of heat in reservoirs 1 and 2,  $J_1 + J_2 = -P < 0$ , in apparent violation of Kelvin's second law.

For example (ii) above,  $T_1 \neq T_2$ , but  $\mu_1 = \mu_2$ . Then Eq. (1) becomes  $J_1(T_1 - T_2) \leq T_1 T_2 \dot{S}_N$  under demon conditions. So when  $\dot{S}_N$  is positive, heat may flow from cold to hot (i.e.,  $J_1$  may have the opposite sign of  $T_2 - T_1$ ), even though no energy comes from the  $N$ -demon, in apparent violation of Clausius's second law.

These arguments show that the demon effects (i) and (ii) do not violate the laws of thermodynamics. Note that, to fix the demon conditions, one requires knowledge of the steady-state flows of charge and energy,  $I_i^E$  and  $I_i$ , but not of the behavior of individual particles. In particular, the  $N$ -demon operates without needing to know about any

microscopic details of the working substance. Once the demon conditions are fixed, the  $N$ -demon generates work, without any further measurement or adjustment.

In the rest of this Letter, we propose two systems which indeed exhibit such effects. Crucially, throughout this Letter, we assume noninteracting particles, which excludes any interpretation in terms of autonomous feedback [6,19–22]. This is the critical difference from a similar setup with strong Coulomb interactions [23], which can be understood as an autonomous Maxwell demon [24].

*Scattering description.*—As there are no interparticle interactions, the setups of interest can be described using scattering theory [25,26], which is known to respect the second law [17,27,28]. The particle and energy currents into reservoir  $i$  are  $I_i = I_i^{(0)}$  and  $I_i^E = I_i^{(1)}$ , where

$$I_i^{(\nu)} = \frac{1}{h} \sum_j \sum_{k,k'} \int dE E^\nu T_{ij}^{kk'}(E) [f_j(E) - f_i(E)]. \quad (2)$$

Here,  $T_{ij}^{kk'}(E)$  are the transmission probabilities from channel  $k'$  in  $j$  to channel  $k$  in  $i$  at energy  $E$ ; see Fig. 1 (superscripts  $k, k'$  are dropped when not relevant). For equilibrium reservoirs,  $f_i(E)$  are Fermi or Bose distributions, depending on the discussed setup. Importantly, the demon effect requires that the nonequilibrium terminal  $N$  has asymmetric and energy-dependent couplings to reservoirs 1 and 2, with  $T_{1N}(E) \neq T_{2N}(E)$  for at least some energy  $E$ . The electronic and optical setups proposed in Fig. 2 fulfill these requirements.

For simplicity, in these setups the nonequilibrium distribution is created from mixing the flows from two equilibrium reservoirs. Note, however, that no spatial separation of these two flows is required. Hence, for clarity,

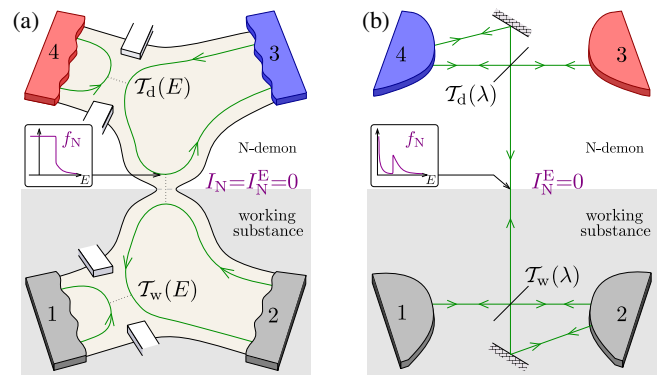


FIG. 2. (a) Electronic, quantum Hall bar (beige) with two constrictions with energy-dependent transmissions  $T_d(E)$  of the  $N$ -demon and  $T_w(E)$  of the working substance. The four reservoirs have different temperatures  $T_i$  and electrochemical potentials  $\mu_i$ . (b) Optical setup with four blackbodies with temperatures  $T_i$  and wavelength-dependent half-silvered mirrors with  $T_d(\lambda)$  and  $T_w(\lambda)$ .

the proposed setups have the demon and the working substance exchanging particles at a single point.

*Proposed implementation 1: Quantum Hall setup.*—As an electronic implementation, we propose a quantum Hall bar in contact with four reservoirs, in which electron transport takes place via chiral edge states [29], marked by green lines with arrows in Fig. 2(a). Such a setup is in experimental reach since effects of nonequilibrium distributions [30] and heat current measurements [31] have been demonstrated. We focus on the  $N$ -demon (reservoirs 3 and 4 together taking the role of the nonequilibrium terminal  $N$  in Fig. 1). The demon is connected by a constriction (with energy-independent transmission, taken for simplicity to be equal to 1) to the working substance, where it generates work as in example (i) above. The work is electrical, with the  $N$ -demon moving electrons against the potential difference  $\mu_2 - \mu_1$  between reservoirs 1 and 2. The nonequilibrium distribution which performs this demonic action is formed using the equilibrium distributions from reservoirs 3 and 4 with possibly different temperatures  $T_{3/4} = T + \delta T_{3/4}$  and electrochemical potentials,  $\mu_{3/4} = \mu + \delta\mu_{3/4}$ . Mixing by an energy-dependent scatterer with transmission  $\mathcal{T}_d(E)$ , yields  $f_N(E) = [1 - \mathcal{T}_d(E)]f_3(E) + \mathcal{T}_d(E)f_4(E)$ . Two of the four parameters ( $\delta T_3$ ,  $\delta T_4$ ,  $\delta\mu_3$ , and  $\delta\mu_4$ ) determine the out of equilibrium distribution, while the other two are tuned to ensure the demon conditions,  $I_3 + I_4 := I_N = 0$  and  $I_3^E + I_4^E := I_N^E = 0$ . These demon conditions are similar to the condition for a voltage or temperature probe [29,32,33], but we repeat that they should not be confused with the measurement-feedback scheme of a standard Maxwell demon.

The energy-dependent transmission asymmetry is done by inserting a scatterer with transmission  $\mathcal{T}_w(E)$ , leading to transmission probabilities  $\mathcal{T}_{14}(E) = \mathcal{T}_d(E)\mathcal{T}_w(E)$  and  $\mathcal{T}_{21}(E) = \mathcal{T}_w(E)$ . In the linear regime (small potential and temperature differences), analytic results are as follows. For affinities  $F_i^\mu = \delta\mu_i/k_B T$  and  $F_i^T = \delta T_i/k_B T^2$ , and defining  $F_{ij}^x = F_i^x - F_j^x$ , the demon conditions imply that

$$F_{32}^\mu = F_3^T \frac{(g_d^1)^2 + g_d^0 X_{0d}^2}{g_0^0 g_d^1} - F_4^T \frac{(g_d^1)^2 - g_d^0 g_d^2}{g_0^0 g_d^1}, \quad (3)$$

and that  $F_{42}^\mu$  takes the same form, with  $g_d^0$  replaced by  $-X_{0d}^0$ . Here,  $X_{\alpha\beta}^\nu = g_\alpha^\nu - g_\beta^\nu$  for  $\alpha, \beta = d, w, 0$ , with  $g_{\alpha\dots\beta}^\nu = (k_B T/h) \int dE (-\partial_E f) E^\nu \mathcal{T}_{\alpha\dots\beta}$  for Fermi function  $f$  and  $\mathcal{T}_0 = 1$ . Then the particle currents are

$$I_1 = -I_2 = g_w^0 F_{21}^\mu + F_3^T \frac{g_0^2 (g_w^0 g_d^0 - g_{dw}^0 g_0^0) + g_0^0 g_w^1 g_d^1}{g_0^0 g_d^1} - F_{43}^T \left( g_w^0 \frac{(g_d^1)^2 - g_d^2 g_d^0}{g_d^1 g_0^0} - \frac{g_d^1 g_{dw}^1 - g_{dw}^0 g_d^2}{g_d^1} \right). \quad (4)$$

The crucial point is that the second and third terms on the right-hand side can overcome the first term such that a

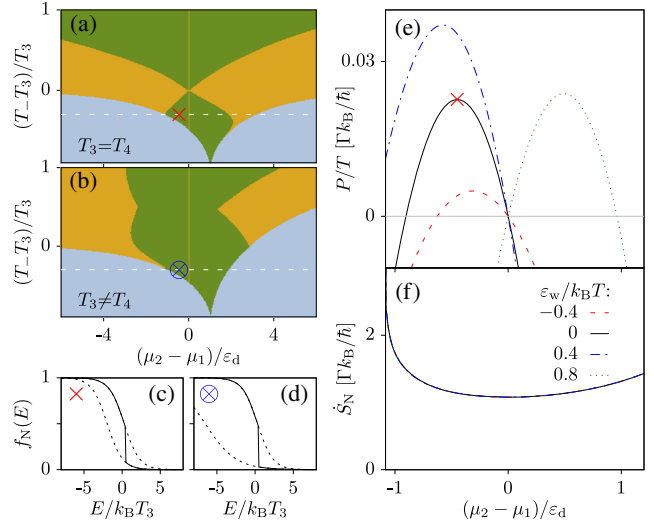


FIG. 3. Power generation in the working substance of the quantum Hall setup.  $\mathcal{T}_d$  is a step function with threshold  $\epsilon_d/k_B T_3 = 0.5$ , and  $\mathcal{T}_w$  has a resonance  $\epsilon_w$  with width  $\Gamma$ . (a)  $T_3 = T_4$ . Map of regions where the demon conditions cannot be fulfilled (cyan), where they can be fulfilled, but no power is generated (yellow), and where power generation with the  $N$ -demon is possible (green). At  $\times$  the  $N$ -demon produces maximum power if  $\epsilon_w = 0$ ; the injected nonequilibrium distribution is shown in (c) compared to  $f_{3/4}(E)$  (dashed lines). (b) Same as (a), with  $T_4 = 2T_3$ . The injected nonequilibrium distribution at  $\otimes$  is shown in (d). (e) Power generated in the working substance and (f) entropy production in the  $N$ -demon, for  $T_3 = T_4 = 7T/10$  [white dashed line in (a)] and different  $\epsilon_w$ .

current flows between reservoirs 1 and 2 against the potential gradient. Algebra shows that this occurs only for transmissions with the properties below Eq. (2).

In stark contrast with known thermoelectric generators [17,18,34], this works even if the working substance is electron-hole symmetric [ $\mathcal{T}_w(E)$  symmetric about  $\mu$ ]. The nonequilibrium distributions break the electron-hole symmetry [via  $\mathcal{T}_d(E)$ ], so one can have finite power output even when  $\mathcal{T}_w(E)$  is symmetric.

Figure 3 presents results for the nonlinear regime, from Eq. (2), for arbitrary  $T_i$  and  $\mu_i$ . We choose the  $N$ -demon's transmission as a quantum point contact,  $\mathcal{T}_d(E) = \theta(E - \epsilon_d)$ , and the working substance's transmission to be that of a weakly coupled quantum dot,  $\mathcal{T}_w(E) = \Gamma^2 / [(E - \epsilon_w)^2 + \Gamma^2]$  with small width  $\Gamma$ . These are experimentally well understood and controllable circuit elements. For fixed  $\mathcal{T}_d$  and temperatures  $T_3$  and  $T_4$ , Figs. 3(a) and 3(b) show the regions where the demon conditions can be met by adjusting  $\mu_3$  and  $\mu_4$  and where power generation is possible with  $\epsilon_w$  tuned to a suitable value with gates. The shape of these maps depends on  $\mathcal{T}_d$ ; however they usually show power generation under demon conditions in an extended parameter regime, even when  $T_3 = T_4$ , so long as  $T_3 \neq T$ ; see Fig. 3(a).

Taking  $T_3 = T_4 = 7T/10$ , Fig. 3(e) shows the power generated as a function of  $\mu_1 - \mu_2$  and for different  $\varepsilon_w$ . For two specific situations, we show the nonequilibrium distribution injected by the  $N$ -demon; see Figs. 3(c) and 3(d). As required by Eq. (1), the entropy production in the  $N$ -demon,  $\dot{S}_N = J_3/T_3 + J_4/T_4$ , is always larger than  $P/T$ ; see Fig. 3(f). However, in contrast to what one would expect from a feedback-based demon [6,19–22], the entropy production of the  $N$ -demon does not depend on the details of the working substance. Importantly, this entropy production is spatially completely separated from the working substance, and its control (or even minimization) is hence of minor relevance.

*Proposed implementation 2: Optical setup.*—Figure 2(b) shows a  $N$ -demon implementation of example (ii) above in an optical setup with noninteracting photons [35]. The demon part of the setup consists of two thermal (blackbody) photon sources at temperatures  $T_3$  and  $T_4$ , emitting light in a wavelength window  $[\lambda_b, \lambda_a]$  (respectively, an energy window  $[E_a, E_b]$  with  $E_{a,b} = hc/\lambda_{a,b}$ ). Both emit photons onto a mirror, which transmits or reflects light in a wavelength-selective manner  $\mathcal{T}_d(\lambda)$ . The resulting nonequilibrium distribution is sent into the lower part of the device, the working substance. The latter consists of two blackbodies with a temperature difference  $\Delta T = T_1 - T_2$ . The relation between temperatures required to satisfy the demon condition,  $I_3^E + I_4^E = 0$ , depends on the  $N$ -demon's transmission  $\mathcal{T}_d(\lambda)$  and the transmission  $\mathcal{T}_w(\lambda)$  of the working substance. In linear response the demon conditions reduce to  $F_3^T = [(g_0^2 - g_w^2)F_1^T + g_w^2 F_2^T - g_d^2 F_4^T]/(g_0^2 - g_d^2)$ , with the same abbreviations as for the electronic setup, but with  $f_i(E) \equiv f_i(hc/\lambda)$  being Bose distributions. Then

$$I_2^E = [AF_{12}^T - g_0^2 g_{dw}^2 F_{14}^T + g_d^2 g_w^2 F_{24}^T]/(g_0^2 - g_d^2), \quad (5)$$

where  $A = g_w^2(2g_0^2 - g_d^2 - g_w^2 + g_{dw}^2)$ . A simple example shows that heat flow between reservoirs 1 and 2 is not always from hotter to colder. Fixing the wavelength-dependent transmissions to be  $\mathcal{T}_d(\lambda) = \theta(\lambda - \lambda_0) = 1 - \mathcal{T}_w(\lambda)$ , we have  $I_2^E \rightarrow g_0^1 F_{12}^T + g_d^1 F_{24}^T$ . Then heat flows from cold to hot when  $F_{12}^T$  and  $F_{24}^T$  have opposite signs, and the magnitude of  $F_{24}^T$  compensates for the difference between  $g_0^1$  and  $g_d^1$ . Figure 4(a) shows the full, nonlinear energy current into reservoir 2 as function of  $T$  and  $\Delta T$ . Cooling of the colder reservoir occurs between the dashed lines. Figures 4(b) and 4(c) show line plots of the cooling power (black lines) for two examples at fixed temperatures  $T$  (indicated by arrows). They also show that the cooling power is enhanced by tuning  $\lambda_0$ . We have assumed that each frequency contributes with a single spatial mode. An increase of the overall cooling power is expected when increasing the mode number.

*Requirements for experimental demonstrations.*—For the quantum Hall implementation of the  $N$ -demon, we expect power outputs of the order of  $P \approx 10$  aW when choosing

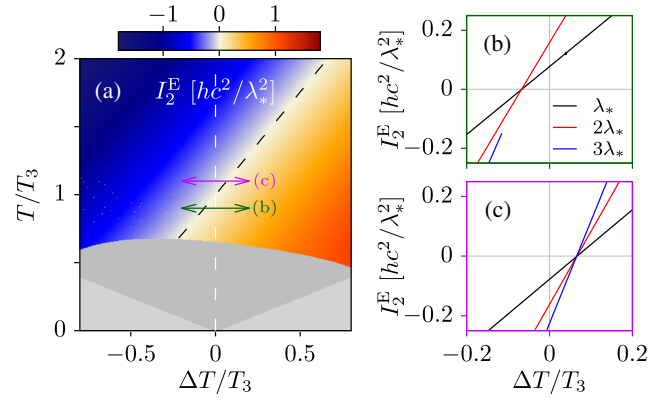


FIG. 4. Optical  $N$ -demon. (a) Cooling power (energy current into reservoir 2) as a function of  $\Delta T$  and  $T$  for  $T_{1(2)} = T \pm \Delta T$ , and fixed  $T_3$ . We set  $\lambda_0 = \lambda_*$ , and  $\lambda_b = 0.02\lambda_*$ ,  $\lambda_a = 5\lambda_*$ .  $T_4$  is given by the demon conditions, which cannot be fulfilled in the dark-gray region (light-gray regions have unphysical negative  $T_{1/2}$ ). White and black dashed lines at  $\Delta T = 0$  and at vanishing cooling power are shown as guides for the eye. The black lines in (b) and (c) show cuts marked by green and magenta arrows at  $T = 0.9T_3$  and  $T = 1.1T_3$ , respectively, together with results for different  $\lambda_0 = 2\lambda_*$ ,  $3\lambda_*$  but the same  $T$  (lines stop when demon conditions are unfulfillable).

$T = 70$  mK,  $T_3 = T_4 = 100$  mK, and  $\Gamma = 1 \mu\text{eV}$  ( $\approx 0.1k_B T$ ). In the optical setup in the near-infrared regime, with wavelengths  $\lambda_d = \lambda_w = 6.2 \mu\text{m}$ ,  $\lambda_a = 12.4 \mu\text{m}$ , and  $\lambda_b = 0.25 \mu\text{m}$  and temperatures around  $T = 1000$  K, the cooling power changes between 0 and  $\pm 0.1 \mu\text{W}$  for temperature gradients between  $\pm 100$  K and 0, respectively. These numbers are experimentally attainable. It is also necessary to experimentally demonstrate that the device is operating under the demon condition. For the electronic setup in Fig. 1(a), a quantum dot with a sharply peaked transmission  $\mathcal{T}_w(E)$  was chosen for the example studied in Fig. 3 because it allows a readout [30] of the incoming nonequilibrium distribution function. An additional side-coupled dot could be used at the outgoing channel from reservoir 2 to 3 to monitor the reinjected equilibrium distribution. In the optical setup the incoming and outgoing light from the  $N$ -demon can be split by a mirror and sent on separate spectrum analyzers. From the detected distribution functions particle and energy currents can be deduced.

*Practical uses.*—Our demons are less intricate to construct than standard Maxwell demons, so their practical uses merit consideration. The implementations that we suggest could be used to spatially separate *production* from *reduction* of entropy for nanoscale heat management. This is a more general version of the nonlocality of thermodynamics laws identified in Ref. [23]. Crucially, if some other independent process generates a nonequilibrium distribution as “waste,” our results show that one can use its nonequilibrium nature as a resource to perform work (or cooling).

*Conclusion.*—We have shown that nonequilibrium distributions can be exploited for power generation and cooling in a demonlike manner. In contrast to other demonlike devices exploiting “engineered reservoirs” (see, e.g., Refs. [36–38]), our proposal does not require any subtle quantum coherence or correlation effects. We have proposed two very different implementations that could be constructed with current technology. For clarity, our two examples have their nonequilibrium distributions made out of two equilibrium reservoirs; however nature is rife with other types of nonequilibrium systems. Our thermodynamics arguments imply that generic nonequilibrium systems could act as  $N$ -demons. It is sufficient that the demon and the working substance exchange energy, similar to Ref. [23]; there is no requirement for the particle exchange. One could also have hybrid systems, e.g., an optical  $N$ -demon acting on an electronic working substance. Transient nonequilibrium effects may also be of interest [39].

We acknowledge our stimulating discussions with the participants of the KITP program “Thermodynamics of Quantum Systems.” This research was supported in part by the National Science Foundation under Grant No. NSF PHY-1748958 (R. S. and J. S.), by the Knut and Alice Wallenberg Foundation and the Swedish Vetenskapsradet VR (J. S.), by the Spanish MINECO via Grant No. FIS2015-74472-JIN (AEI/FEDER/UE), the MAT2016-82015-REDT network and the program MDM-2014-0377, and the Ramón y Cajal program RYC-2016-20778 (R. S.), and by the French ANR-15-IDEX-02 via the Université Grenoble Alpes QuEnG project (R. S. W.).

- 
- [1] See, e.g., the quotes from two letters from Maxwell to Tait (the first on December 11, 1867, and the second undated) in C. G. Knott, *Life and Scientific Work of Peter Guthrie Tait* (Cambridge University Press, Cambridge, England, 1911), pp. 213–215.
- [2] C. H. Bennett, The thermodynamics of computation—A review, *Int. J. Theor. Phys.* **21**, 905 (1982).
- [3] R. Landauer, Irreversibility and heat generation in the computing process, *IBM J. Res. Dev.* **5**, 183 (1961).
- [4] J. V. Koski, V. F. Maisi, T. Sagawa, and J. P. Pekola, Experimental Observation of the Role of Mutual Information in the Nonequilibrium Dynamics of a Maxwell Demon, *Phys. Rev. Lett.* **113**, 030601 (2014).
- [5] J. V. Koski, V. F. Maisi, J. P. Pekola, and D. V. Averin, Experimental realization of a Szilard engine with a single electron, *Proc. Natl. Acad. Sci. U.S.A.* **111**, 13786 (2014).
- [6] J. V. Koski, A. Kutvonen, I. M. Khaymovich, T. Ala-Nissila, and J. P. Pekola, On-Chip Maxwell’s Demon as an Information-Powered Refrigerator, *Phys. Rev. Lett.* **115**, 260602 (2015).
- [7] K. Chida, S. Desai, K. Nishiguchi, and A. Fujiwara, Power generator driven by Maxwell’s demon, *Nat. Commun.* **8**, 15310 (2017).
- [8] N. Cottet, S. Jezouin, L. Bretheau, P. Campagne-Ibarcq, Q. Ficheux, J. Anders, A. Auffèves, R. Azouit, P. Rouchon, and B. Huard, Observing a quantum Maxwell demon at work, *Proc. Natl. Acad. Sci. U.S.A.* **114**, 7561 (2017).
- [9] Y. Masuyama, K. Funo, Y. Murashita, A. Noguchi, S. Kono, Y. Tabuchi, R. Yamazaki, M. Ueda, and Y. Nakamura, Information-to-work conversion by Maxwell’s demon in a superconducting circuit quantum electrodynamical system, *Nat. Commun.* **9**, 1291 (2018).
- [10] M. D. Vidrighin, O. Dahlsten, M. Barbieri, M. S. Kim, V. Vedral, and I. A. Walmsley, Photonic Maxwell’s Demon, *Phys. Rev. Lett.* **116**, 050401 (2016).
- [11] P. A. Camati, J. P. S. Peterson, T. B. Batalhão, K. Micadei, A. M. Souza, R. S. Sarthour, I. S. Oliveira, and R. M. Serra, Experimental Rectification of Entropy Production by Maxwell’s Demon in a Quantum System, *Phys. Rev. Lett.* **117**, 240502 (2016).
- [12] V. Serreli, C.-F. Lee, E. R. Kay, and D. A. Leigh, A molecular information ratchet, *Nature (London)* **445**, 523 (2007).
- [13] S. Toyabe, T. Sagawa, M. Ueda, E. Muneyuki, and M. Sano, Experimental demonstration of information-to-energy conversion and validation of the generalized Jarzynski equality, *Nat. Phys.* **6**, 988 (2010).
- [14] A. Bérut, A. Arakelyan, A. Petrosyan, S. Ciliberto, R. Dillenschneider, and E. Lutz, Experimental verification of Landauer’s principle linking information and thermodynamics, *Nature (London)* **483**, 187 (2012).
- [15] É. Roldán, I. A. Martínez, J. M. R. Parrondo, and D. Petrov, Universal features in the energetics of symmetry breaking, *Nat. Phys.* **10**, 457 (2014).
- [16] We use the word “terminal” for  $N$  because “reservoir” often implies internal equilibrium, which is not appropriate for  $N$ .
- [17] G. Benenti, G. Casati, K. Saito, and R. S. Whitney, Fundamental aspects of steady-state conversion of heat to work at the nanoscale, *Phys. Rep.* **694**, 1 (2017).
- [18] R. S. Whitney, R. Sánchez, and J. Splettstoesser, Quantum thermodynamics of nanoscale thermoelectrics and electronic devices, in *Thermodynamics in the Quantum Regime: Fundamental Aspects and New Directions*, edited by F. Binder, L. A. Correa, C. Gogolin, J. Anders, and G. Adesso (Springer, Cham, Switzerland, 2018), pp. 175–206.
- [19] M. Esposito and G. Schaller, Stochastic thermodynamics for “Maxwell demon” feedbacks, *Europhys. Lett.* **99**, 30003 (2012).
- [20] P. Strasberg, G. Schaller, T. Brandes, and M. Esposito, Thermodynamics of a Physical Model Implementing a Maxwell Demon, *Phys. Rev. Lett.* **110**, 040601 (2013).
- [21] A. C. Barato and U. Seifert, An autonomous and reversible Maxwell’s demon, *Europhys. Lett.* **101**, 60001 (2013).
- [22] N. Shiraishi, S. Ito, K. Kawaguchi, and T. Sagawa, Role of measurement-feedback separation in autonomous Maxwell’s demons, *New J. Phys.* **17**, 045012 (2015).
- [23] R. S. Whitney, R. Sánchez, F. Haupt, and J. Splettstoesser, Thermoelectricity without absorbing energy from the heat sources, *Physica E* **75**, 257 (2016).
- [24] R. Sánchez, P. Samuelsson, and P. P. Potts, Autonomous conversion of information to work in quantum dots, *Phys. Rev. Res.* **1**, 033066 (2019).

- [25] P.N. Butcher, Thermal and electrical transport formalism for electronic microstructures with many terminals, *J. Phys. Condens. Matter* **2**, 4869 (1990).
- [26] M. Büttiker, Scattering theory of current and intensity noise correlations in conductors and wave guides, *Phys. Rev. B* **46**, 12485 (1992).
- [27] G. Nenciu, Independent electron model for open quantum systems: Landauer-Büttiker formula and strict positivity of the entropy production, *J. Math. Phys. (N.Y.)* **48**, 033302 (2007).
- [28] R.S. Whitney, Thermodynamic and quantum bounds on nonlinear dc thermoelectric transport, *Phys. Rev. B* **87**, 115404 (2013).
- [29] M. Büttiker, Absence of backscattering in the quantum Hall effect in multiprobe conductors, *Phys. Rev. B* **38**, 9375 (1988).
- [30] C. Altimiras, H. le Sueur, U. Gennser, A. Cavanna, D. Mailly, and F. Pierre, Non-equilibrium edge-channel spectroscopy in the integer quantum Hall regime, *Nat. Phys.* **6**, 34 (2010).
- [31] S. Jezouin, F.D. Parmentier, A. Anthore, U. Gennser, A. Cavanna, Y. Jin, and F. Pierre, Quantum limit of heat flow across a single electronic channel, *Science* **342**, 601 (2013).
- [32] M. Büttiker, Four-Terminal Phase-Coherent Conductance, *Phys. Rev. Lett.* **57**, 1761 (1986).
- [33] M. Büttiker, Coherent and sequential tunneling in series barriers, *IBM J. Res. Dev.* **32**, 63 (1988).
- [34] R. Sánchez, B. Sothmann, and A. N. Jordan, Chiral Thermoelectrics with Quantum Hall Edge States, *Phys. Rev. Lett.* **114**, 146801 (2015).
- [35] The constraint of zero particle flow is dropped here because photons are not conserved in the reservoirs, so they have zero chemical potential. This means that particle flow cannot affect the thermodynamics of heat and work.
- [36] M. O. Scully, M. S. Zubairy, G. S. Agarwal, and H. Walther, Extracting work from a single heat bath via vanishing quantum coherence, *Science* **299**, 862 (2003).
- [37] G. Francica, J. Goold, F. Plastina, and M. Paternostro, Daemonic ergotropy: Enhanced work extraction from quantum correlations, *npj Quantum Inf.* **3**, 12 (2017).
- [38] A. Ghosh, W. Niedenzu, V. Mukherjee, and G. Kurizki, Thermodynamic principles and implementations of quantum machines, in *Thermodynamics in the Quantum Regime: Fundamental Aspects and New Directions*, edited by F. Binder, L. A. Correa, C. Gogolin, J. Anders, and G. Adesso (Springer, Cham, Switzerland, 2018), pp. 37–66.
- [39] M. Konopik, A. Friedenberger, N. Kiesel, and E. Lutz, Nonequilibrium information erasure below  $kT \ln 2$ , *arXiv*: 1806.01034.